# Threshold States

A. Tohsaki (信州)
P. Schuck (Orsay)
G. Röpke (Rostock)
Y. Funaki (京大)
H. H.

- 序論
- $\alpha$ condensation in $^{12}C$ and $^{16}O$
- deformed condensate of $\alpha$
  study of $^{8}Be$
- summarizing discussion

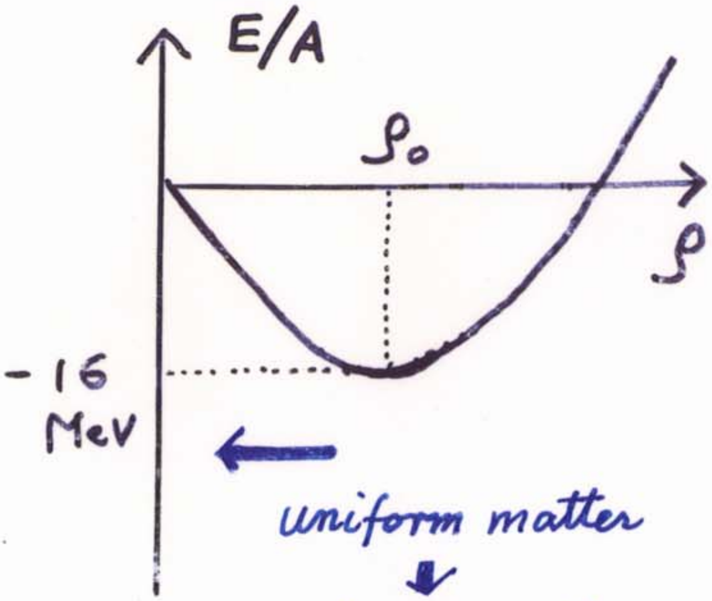


uniform matter

⇓

cluster matter

$\frac{E_\alpha}{4} \approx -7$ MeV

Boson cluster

⇓

Bose-Einstein condensation

In finite nuclei

$(E/A)_{\substack{\text{stable}\\ \text{nuclei}}} \approx -8$ MeV

$(E_\alpha/4) \approx -7$ MeV

- mean field character
- clustering character

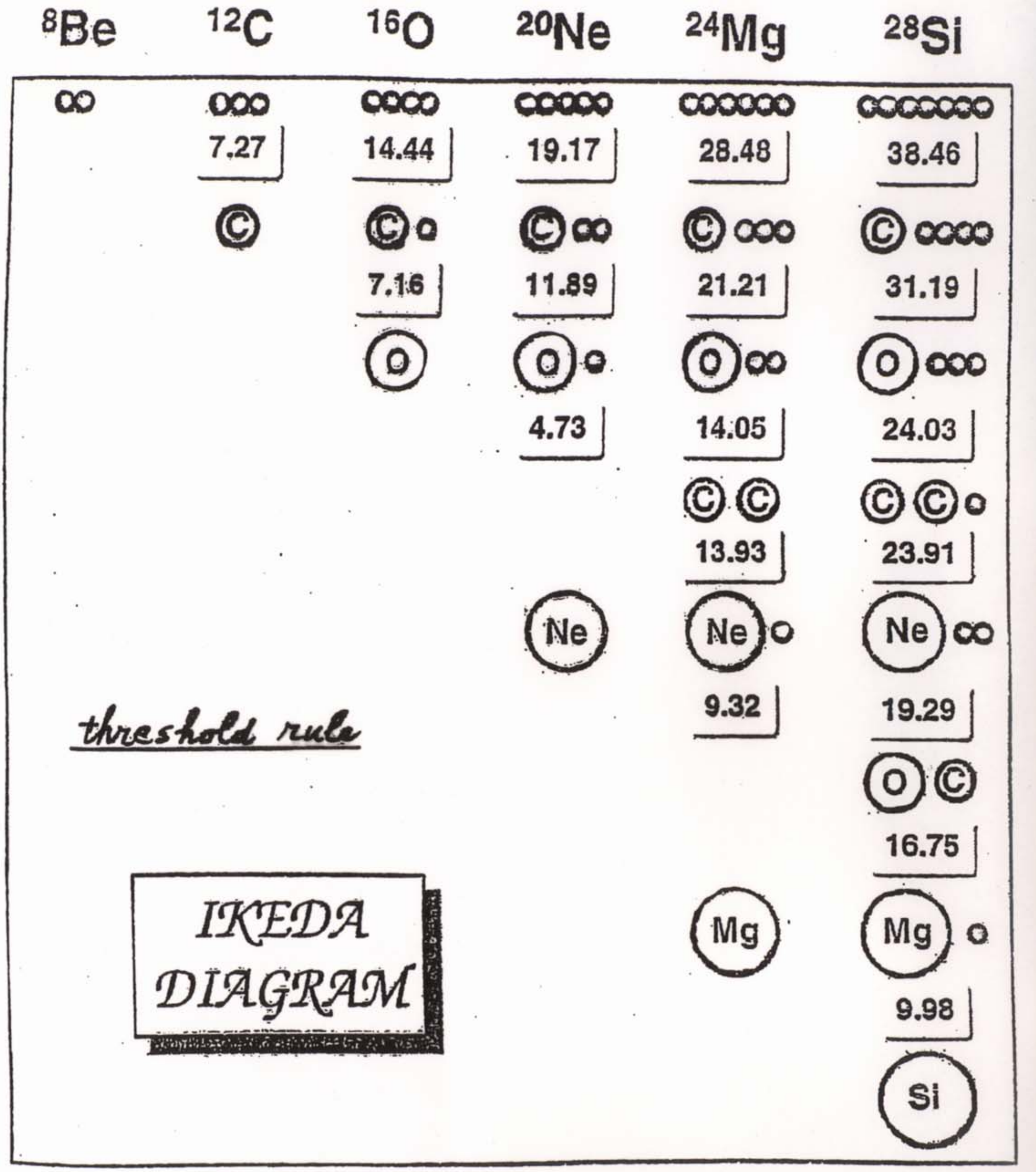


FIG. 43. Ikeda diagram for light nuclei. The threshold energy for each decay mode (in MeV) is indicated (Horiuchi *et al.*, 1972).

P. A. Butler & W. Nazarewicz
Rev. Mod. Phys. 68, No. 2, 349 (1996)

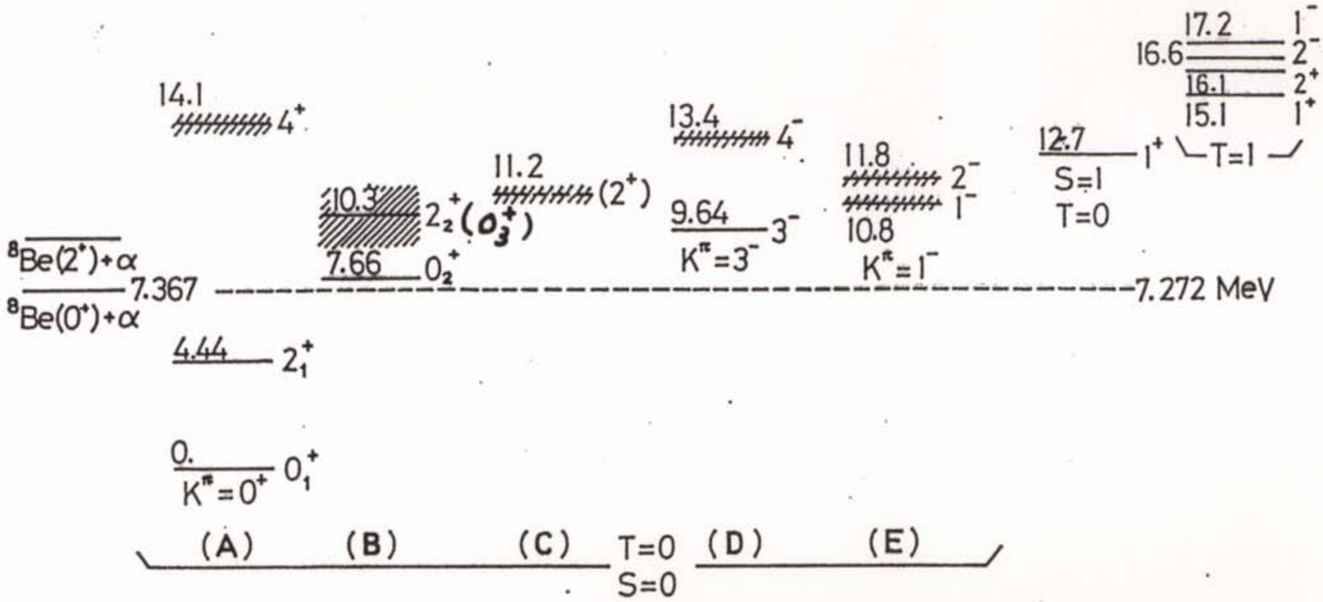


Fig. 1-1. Experimental energy levels of $^{12}$C are classified into several bands according to the dynamical calculations in § 2. (A) $K^\pi=0^+$ ground rotational band, (B) the first family of the excited positive-parity states including the $0_2{}^+$ and $2_2{}^+$ states, (C) the second family of excited positive-parity states. (D) shows $K^\pi=3^-$ band, (E) $K^\pi=1^-$ band. The data are taken from Ref. 16). Here, the $(0^+)$ level at 10.3 MeV and the $(2^-)$ level at 13.35 MeV are assigned to $J^\pi=2^+$ and $4^-$ respectively, according to the dynamical calculations in § 2.

Coexistence of states
with mean field structure
and
with cluster structure

"Alpha condensation"

A. Tohsaki
P. Schuck
G. Röpke
H.H.

Phys. Rev. Letters 87 (2001), 192501.

What kind of cluster structure can be expected near $n\alpha$ threshold ?

$n\alpha$ linear chain ?

H. Morinaga

For $3\alpha$, linear chain structure is not supported by the solution of $3\alpha$ problem.

the observed $0^+$ state near $3\alpha$ threshold can be described approximately

$$\Phi_{0_2^+}(3\alpha) \approx \mathcal{A}\left\{ e^{-\gamma(X_{\alpha_1}^2+X_{\alpha_2}^2+X_{\alpha_3}^2)}\, \Phi_\alpha \Phi_\alpha \Phi_\alpha \right\}$$

$\gamma$ = small : low density

$3\alpha$ particles occupy the same $0s$ orbit $e^{-\gamma X^2}$.

P.T.P. Supple. 68
Chapt. 2



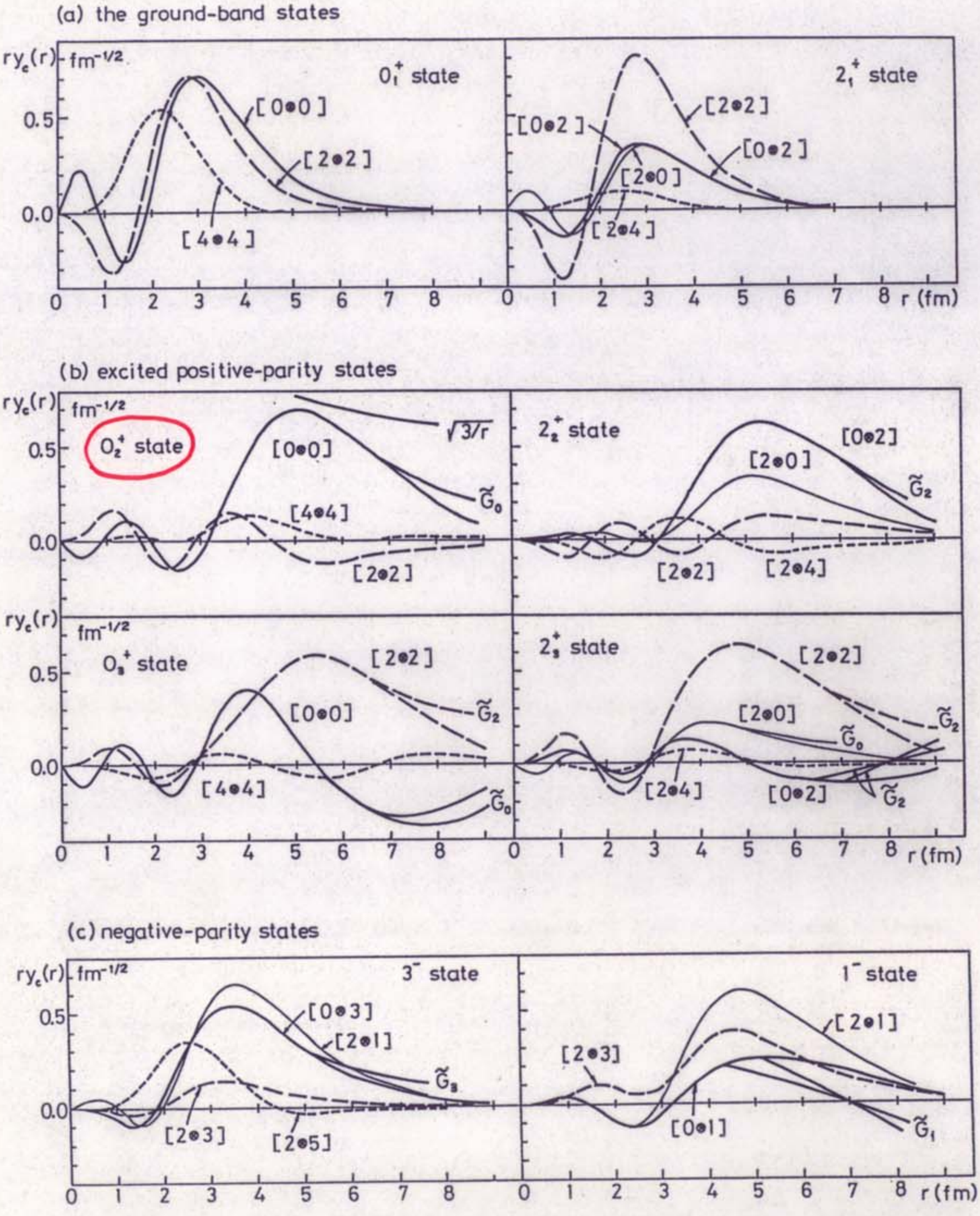


Fig. 2-7. $\alpha$-reduced width amplitudes $ry_c(r)$ and connected resonance tails $\tilde{G}_l(kr)$. Bracket $[I\otimes l]$ denotes a spin of $^8$Be core $I$ and an orbital angular momentum of the $\alpha$-particle $l$, specifying the channel.

should be recognized here that each state has its own single dominant amplitude. According to them, we can classify the states into two groups; one includes the $0_2^+$ and $2_2^+$ states, the other does the $0_3^+$ and $2_3^+$ states. In the former an $\alpha$-particle interacts mainly with the $^8$Be ground state, while in the latter it interacts with the first excited state of $^8$Be (the $2_1^+$ at 2.94 MeV).

P.T.P. Supple. 68
Chapt. 2

## 2.2. *Energy spectra and structure of* $^{12}$C

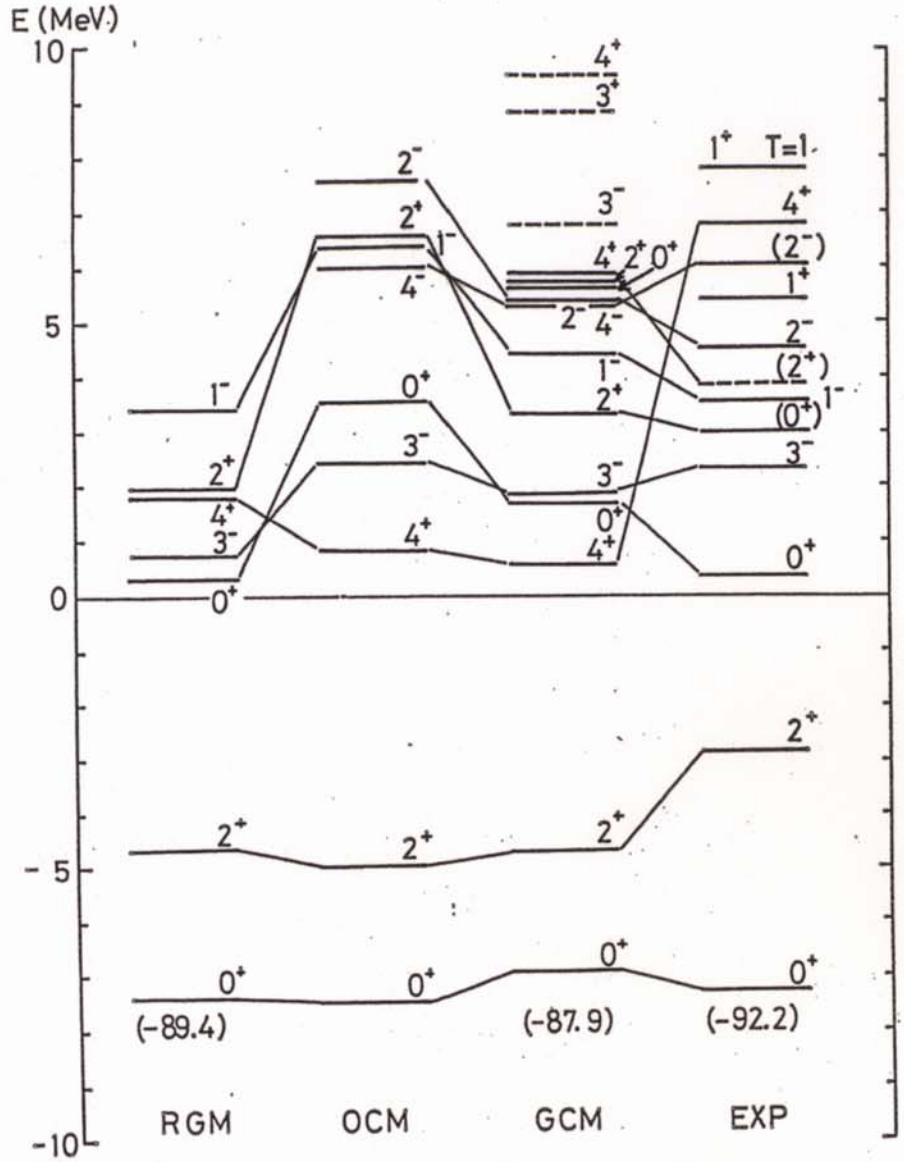


Fig. 2-2. Calculated energy spectra of $^{12}$C and the experimental one.[16] The result of the OCM is taken from Ref. 36). Nucleon-nucleon interactions in Table 2-II are used with the Coulomb interaction. In the RGM and GCM cases, calculated $3\alpha$ energies are subtracted from the total energies, while the total energies of the ground state are given in parentheses under the levels, respectively.

< $n\alpha$ "condensed state" >

$$|\Phi_{n\alpha}\rangle = (C_\alpha^\dagger)^n |0\rangle$$

$$C_\alpha^\dagger \equiv \int d^3R\, e^{-R^2/\beta^2}\, B_\alpha^\dagger(\vec{R})$$

$$B_\alpha^\dagger(\vec{R}) \equiv b_{p\uparrow}^\dagger(\vec{R})\, b_{p\downarrow}^\dagger(\vec{R})\, b_{n\uparrow}^\dagger(\vec{R})\, b_{n\downarrow}^\dagger(\vec{R})$$

$$b_i^\dagger(\vec{R}) \equiv \int d^3r\, \underbrace{\varphi_{0s}(\vec{r}-\vec{R})}_{\left(\frac{1}{\pi b^2}\right)^{\frac{3}{4}} e^{-\frac{1}{2b^2}(\vec{r}-\vec{R})^2}}\, a_i^\dagger(\vec{r})$$

$$\{a_i^\dagger(\vec{r}),\, a_j^\dagger(\vec{r}')\} = 0$$

$$\{a_i(\vec{r}),\, a_j^\dagger(\vec{r}')\} = \delta_{ij}\, \delta(\vec{r}-\vec{r}')$$

$$\langle \vec{r}_1 i_1, \cdots, \vec{r}_4 i_4 |\, B_\alpha^\dagger(\vec{R}) |0\rangle \propto \det \left| (\varphi_{0s}(\vec{r}-\vec{R}))^4 \right|$$

$$\propto e^{-\frac{2}{b^2}(\vec{X}-\vec{R})^2}\, \phi(\alpha)$$

$$(i_1, \cdots, i_4) = (p\uparrow, p\downarrow, n\uparrow, n\downarrow)$$

$$\vec{X} \equiv (\vec{r}_1 + \vec{r}_2 + \vec{r}_3 + \vec{r}_4)/4$$

$$\langle \vec{r}_1 i_1, \cdots, \vec{r}_4 i_4 | \, C_\alpha^+ \, | 0 \rangle$$

$$\propto \int d^3R \; e^{-\frac{R^2}{\beta^2}} \; \det \left| \left( \varphi_{0s}(\vec{r}-\vec{R}) \right)^4 \right|$$

$$\propto e^{-\frac{2}{B^2} X^2} \phi(\alpha)$$

$$B^2 \equiv b^2 + 2\beta^2$$

$$\langle \vec{r}_1 i_1, \cdots, \vec{r}_{4n} i_{4n} | \, (C_\alpha^+)^n \, | 0 \rangle$$

$$\propto \int d^3R_1 \cdots d^3R_n \; e^{-\frac{1}{\beta^2}(R_1^2 + \cdots + R_n^2)}$$

$$\times \det \left| \left( \varphi_{0s}(\vec{r}-\vec{R}_1) \right)^4 \cdots \left( \varphi_{0s}(\vec{r}-\vec{R}_n) \right)^4 \right|$$

$$\propto \mathcal{A} \left\{ e^{-\frac{2}{B^2}(X_1^2 + \cdots + X_n^2)} \phi(\alpha_1) \cdots \phi(\alpha_n) \right\}$$

$$|\Phi^N_{3\alpha}\rangle \xrightarrow[R_0\to 0]{} |(0s)^4(0p)^8\,[444]\,0^+\rangle$$

$$|\Phi^N_{4\alpha}\rangle \xrightarrow[R_0\to 0]{} |(0s)^4(0p)^{12}\,0^+\rangle$$

double closed shell

$$|\Phi^N_{n\alpha}\rangle \equiv |\Phi_{n\alpha}\rangle \Big/ \sqrt{\langle\Phi_{n\alpha}|\Phi_{n\alpha}\rangle}$$

Energy surface

$$\langle \Phi^N_{n\alpha}(R_0,b) \,|\, H \,|\, \Phi^N_{n\alpha}(R_0,b)\rangle$$

Generator coordinate method

$$\sum_j \left\langle \Phi^N_{n\alpha}((R_0,b)_i) \right| (H-E_k) \left| \Phi^N_{n\alpha}((R_0,b)_j) \right\rangle f_k((R_0,b)_j) = 0$$

$$|\Psi_{n\alpha,k}\rangle = \sum_j f_k((R_0,b)_j)\,|\Phi^N_{n\alpha}((R_0,b)_j)\rangle$$

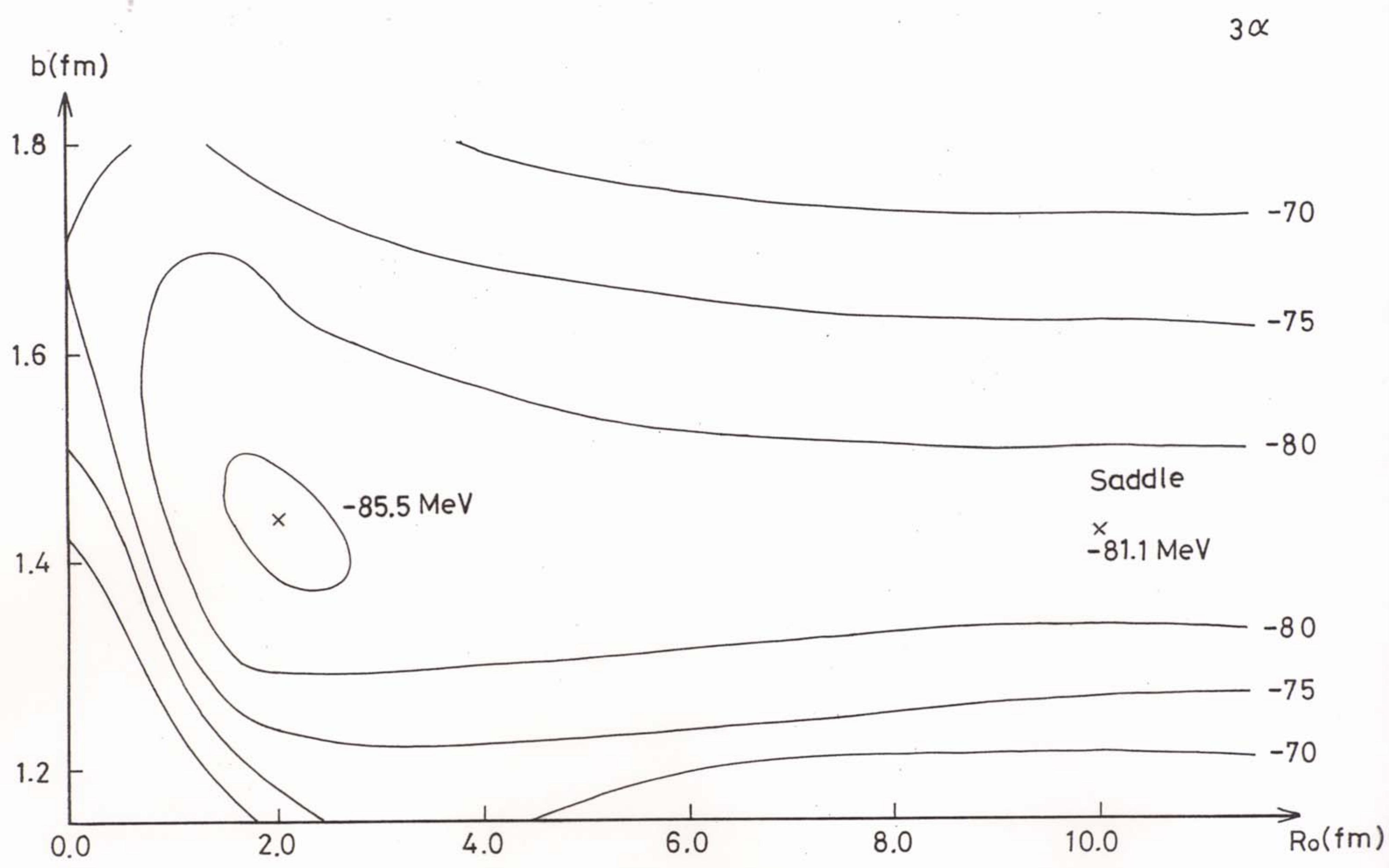
3α
b(fm)
1.8
1.6
1.4
1.2
0.0
2.0
4.0
6.0
8.0
10.0
Ro(fm)
-70
-75
-80
-85.5 MeV
Saddle
-81.1 MeV
-80
-75
-70

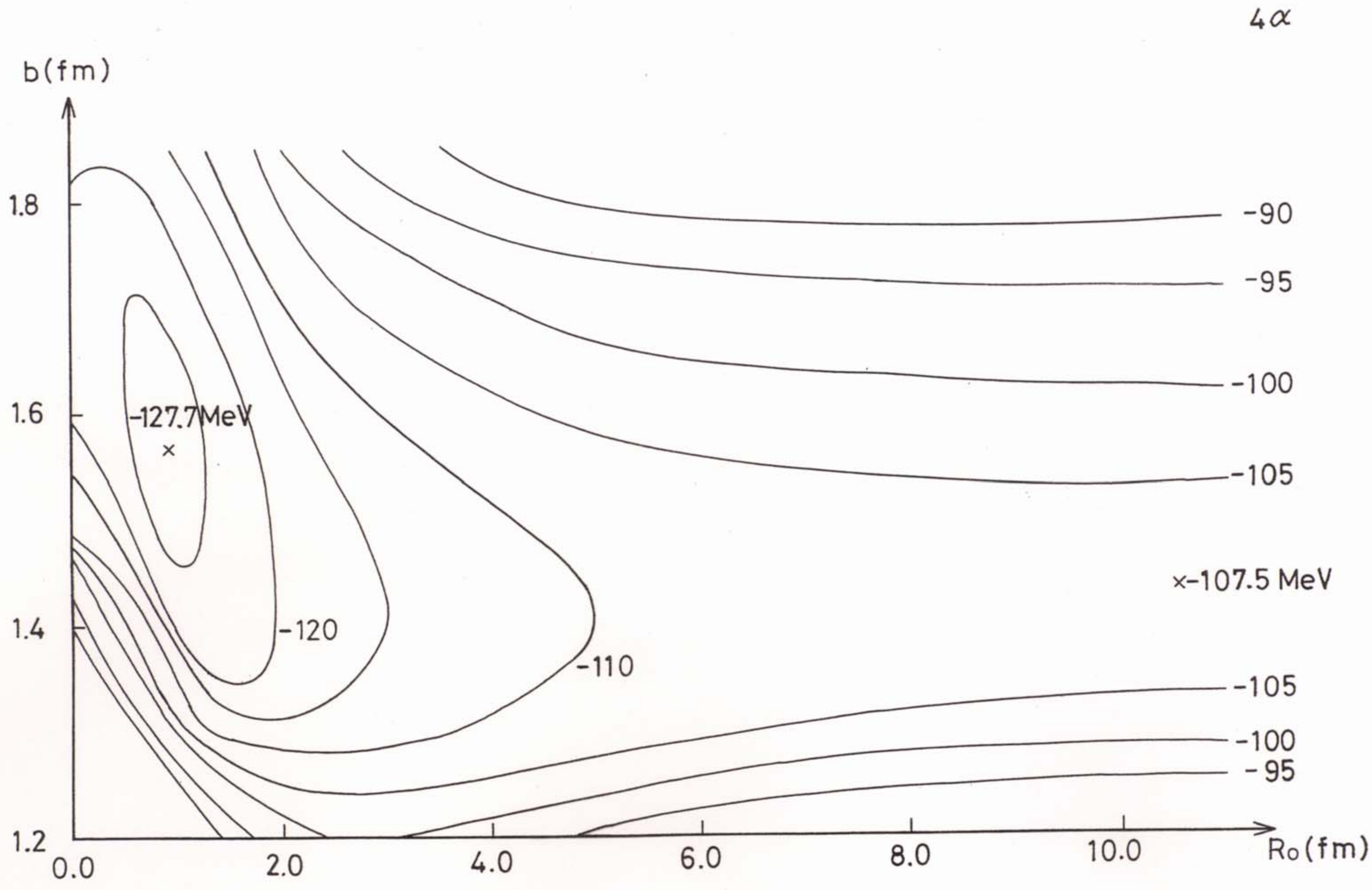
4α
b(fm)
1.8
1.6
1.4
1.2
0.0
2.0
4.0
6.0
8.0
10.0
R₀(fm)
-127.7MeV
-120
-110
-90
-95
-100
-105
×-107.5 MeV
-105
-100
-95

| | | $E_k - E_{thr}$ (MeV) | $(E - E_{thr})_{exp}$ (MeV) | $\sqrt{\langle r^2 \rangle}$ (fm) | $(\sqrt{\langle r^2 \rangle})_{exp}$ (fm) |
|---|---|---|---|---|---|
| $^{12}C$ | $k=1$ $(0_1^+)$ | $-3.4$ | $-7.27$ | 2.97 | 2.65 |
| | $k=2$ $(0_2^+)$ | $\boxed{+0.5}$ | $\boxed{+0.38}$ | 4.29 | |
| $^{16}O$ | $k=1$ $(0_1^+)$ | $-14.8$ | $-14.44$ | 2.59 | 2.73 |
| | $k=2$ $(0_3^+)$ | $-6.0$ | $-3.18$ | 3.16 | |
| | $k=3$ $(0_5^+)$ | $\boxed{-0.7}$ | $\boxed{-0.44}$ | 3.97 | |

$\rho \sim \frac{1}{3}\rho_0$

<Observed lowest $0^+$ states>

| | | $E_x$ (MeV) | $\Gamma$ (MeV) |
|---|---|---|---|
| $^{12}C$ | $0_1^+$ | 0.0 | |
| | $0_2^+$ | 7.66 | $8.7 \times 10^{-6}$ |
| $^{16}O$ | $0_1^+$ | 0.0 | |
| | $0_2^+$ | 6.06 | |
| | $0_3^+$ | 11.26 | 2.6 |
| | $0_4^+$ | 12.05 | $1.6 \times 10^{-3}$ |
| | $0_5^+$ | 14.0 | 4.8 |
| | $0_6^+$ | 14.03 | $2.0 \times 10^{-1}$ |

## < deformed condensate >

球形 $$C_\alpha^+ = \int d^3R \, e^{-\frac{R^2}{\beta^2}} B_\alpha^+(\vec{R})$$

↓

変形 $$C_\alpha^+ = \int d^3R \, e^{-\frac{R_x^2}{\beta_x^2} - \frac{R_y^2}{\beta_y^2} - \frac{R_z^2}{\beta_z^2}} B_\alpha^+(\vec{R})$$

$$\langle \vec{r}_1 i_1, \cdots, \vec{r}_{4n} i_{4n} | (C_\alpha^+)^n | 0 \rangle$$

$$\propto \mathcal{A}\left\{ \left( \prod_{i=1}^{n} e^{-\frac{2}{B_x^2} X_{ix}^2 - \frac{2}{B_y^2} X_{iy}^2 - \frac{2}{B_z^2} X_{iz}^2} \right) \phi(\alpha_1) \cdots \phi(\alpha_n) \right\}$$

deformed orbit $e^{-\frac{2}{B_x^2} X_x^2 - \frac{2}{B_y^2} X_y^2 - \frac{2}{B_z^2} X_z^2}$

に $n$ ケの $\alpha$ 粒子が凝縮

## 角運動量射影

$$\int d\Omega \, D_{MK}^{J*}(\Omega) \hat{R}(\Omega) \langle \vec{r}_1 i_1 \cdots \vec{r}_{4n} i_{4n} | (C_\alpha^+)^n | 0 \rangle$$

$^8Be$ 2α系

$$\mathcal{A}\left\{ e^{-\frac{r_x^2+r_y^2}{B_x^2}-\frac{r_z^2}{B_z^2}} \phi(\alpha_1)\phi(\alpha_2)\right\}$$

$$\vec{r} \equiv \vec{X}_1 - \vec{X}_2$$

2α系の関数空間

$$\mathcal{A}\left\{ \chi(\vec{r})\phi(\alpha_1)\phi(\alpha_2)\right\}$$

$$\langle \phi(\alpha_1)\phi(\alpha_2) | (H-E) | \mathcal{A}\{\chi(\vec{r})\phi(\alpha_1)\phi(\alpha_2)\}\rangle = 0$$

Resonating Group Method

$$\downarrow\uparrow$$

$$\int d^3R \langle \Phi^B(\vec{R}') | (H-E) | \Phi^B(\vec{R})\rangle f(\vec{R}) = 0$$

Generator Coordinate Method

$$\Phi^B(\vec{R}) = \det\left\{ (\varphi_{0s}(\vec{r}-\tfrac{\vec{R}}{2}))^4 (\varphi_{0s}(\vec{r}+\tfrac{\vec{R}}{2}))^4 \right\}$$

$$\chi(\vec{r}) = \int d^3R \, e^{-\frac{1}{b^2}(\vec{r}-\vec{R})^2} f(\vec{R})$$

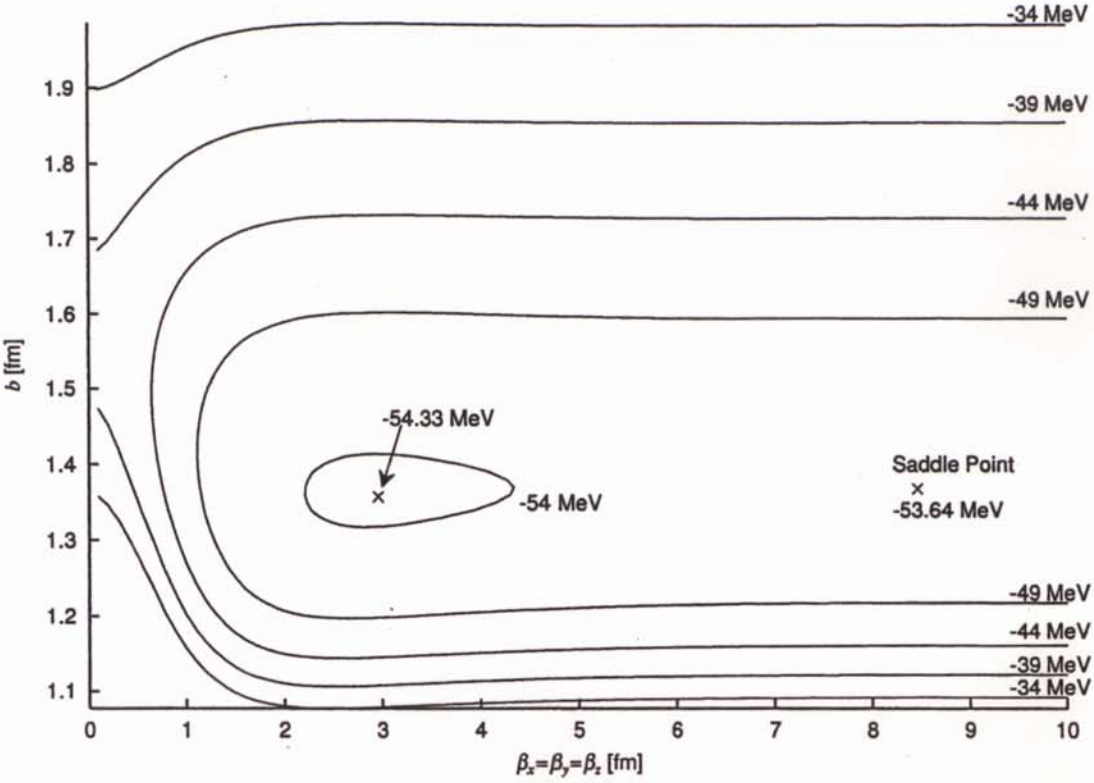


Figure 1: energy surface of spherical case ($M = 0.56$)

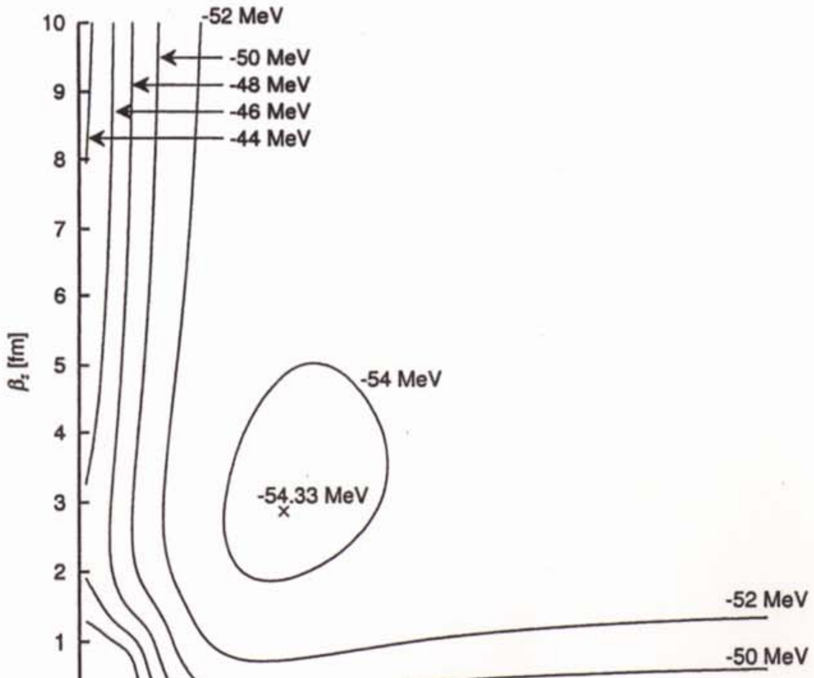


Figure 2: energy surface of deformed case ($M = 0.56$)

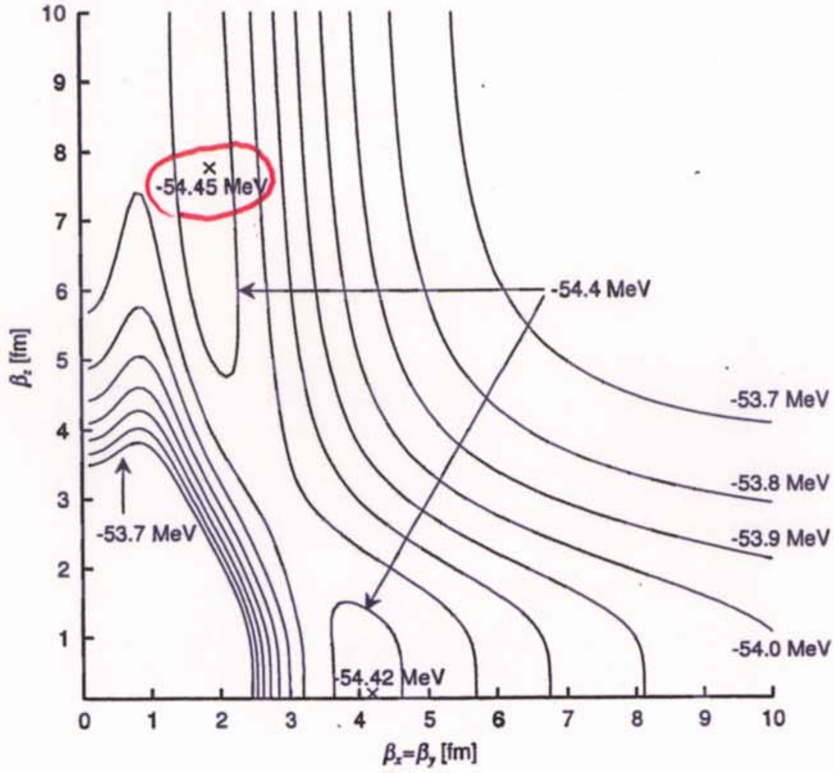


Figure 3: energy surface of $0^+$ w.f ($M = 0.56$)

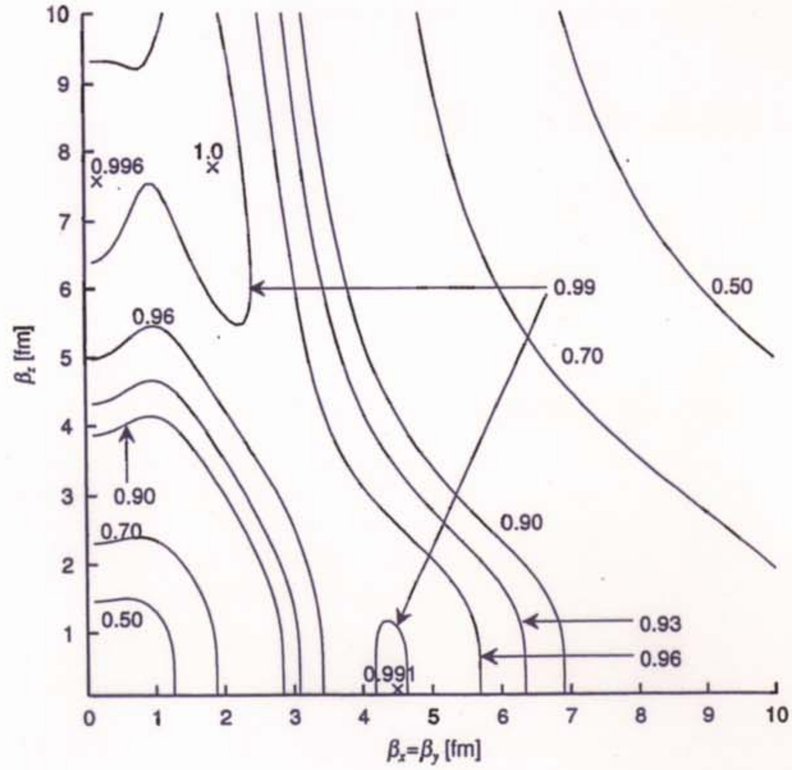


Figure  : overlap surface of $0^+$ with respect to $\beta_x = \beta_y = 1.8$, $\beta_z = 7.8$
4 (a)

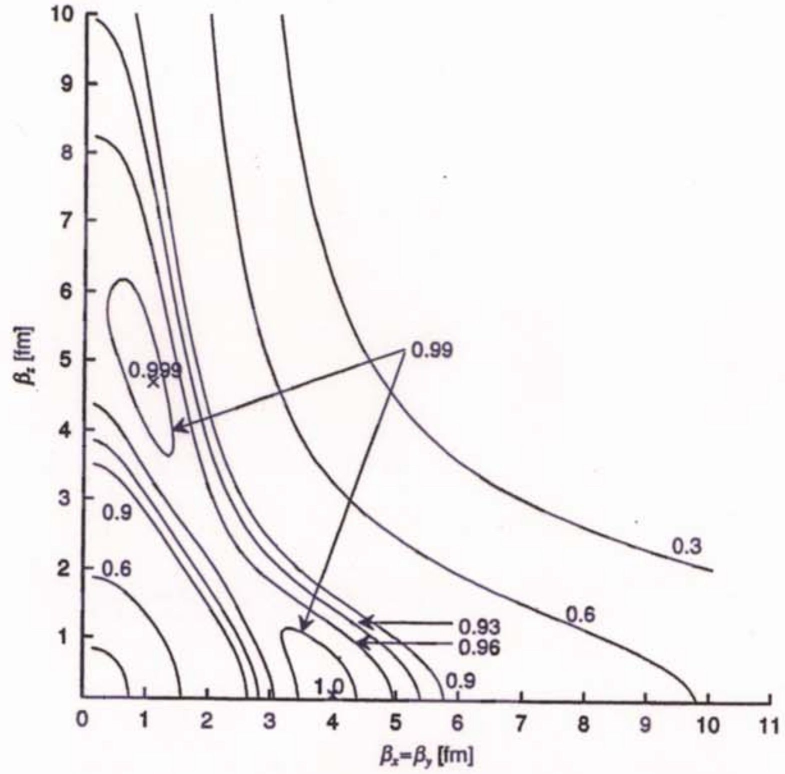


Figure ⁚: overlap surface of $2^+$ with respect to $\beta_x = \beta_y = 3.9\,\beta_z = 0.0$

4 (b)

$$\begin{array}{r} 54.45 \\ -)\ 51.5 \\ \hline 2.95 \end{array} \qquad \begin{array}{r} 54.45 \\ -)\ 51.2 \\ \hline 3.25 \end{array}$$

$(Ex(2^+))_{実} = 2.90$ MeV

$(\Gamma(2^+))_{実} = 1.45$ MeV

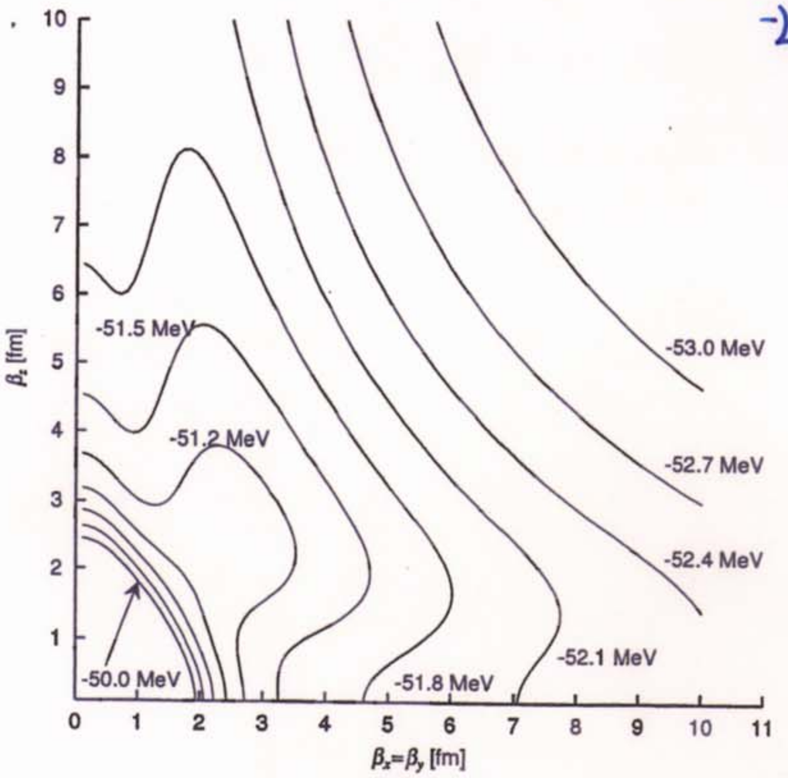


Figure : energy surface of $2^+$ w.f ($M = 0.56$)

5

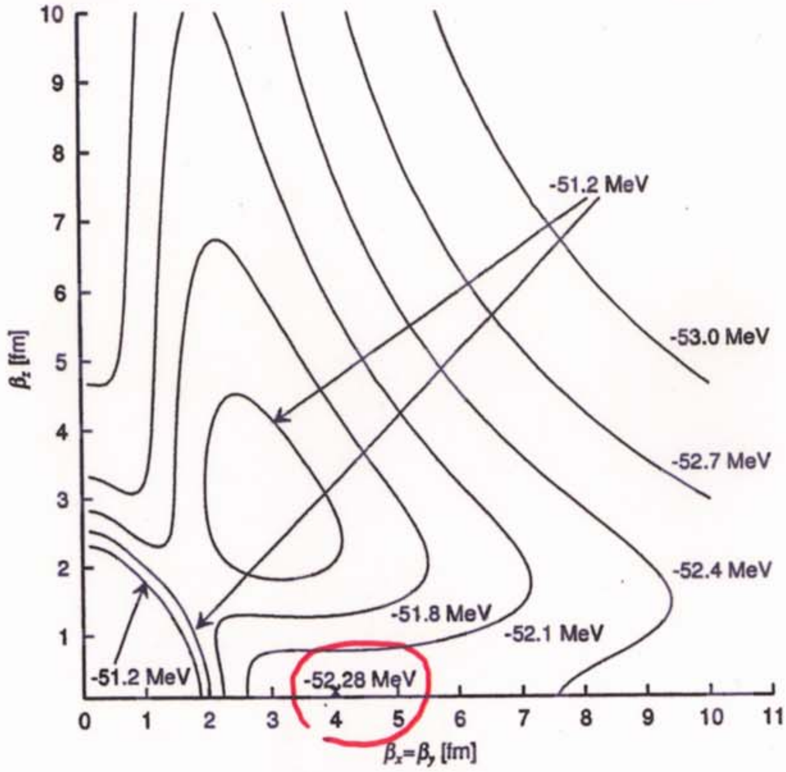


Figure 6 : energy surface of $2^+$ w.f ($M = 0.54$)

$$
\begin{array}{r}
55.19 \\
-)\ 52.28 \\
\hline
2.91
\end{array}
$$

$(E_x(2^+))_{実} = 2.90$ MeV

$(\Gamma(2^+))_{実} = 1.45$ MeV

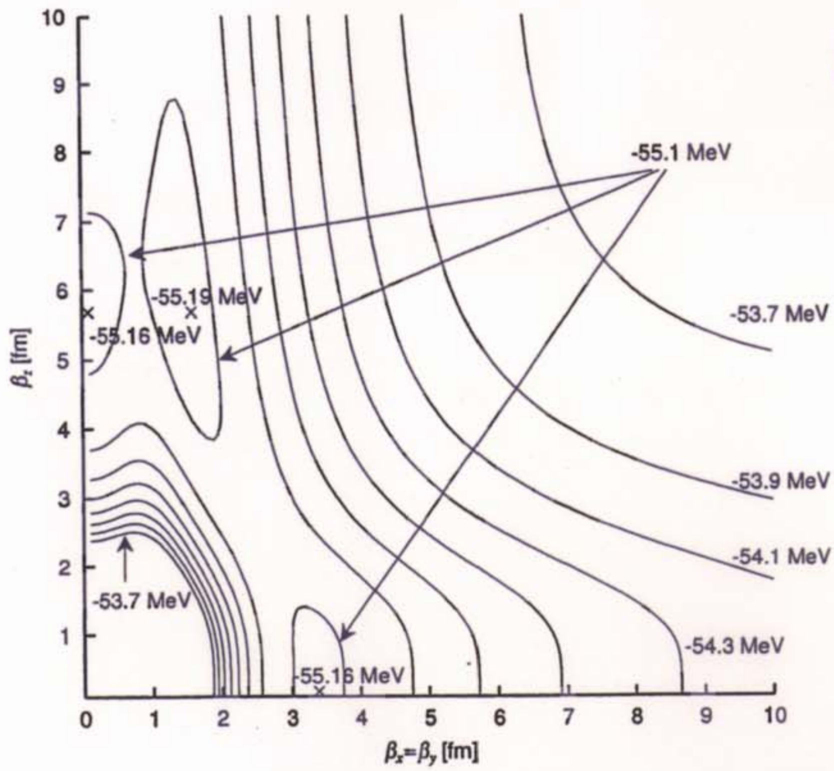


Figure 7 : energy surface of $0^+$ w.f ($M = 0.54$)

$$\sum_j \langle \Phi^{BO^+}(R_i) | (H-E) | \Phi^{BO^+}(R_j) \rangle f(R_j) = 0$$

$$\Phi^{BO^+}(R) \equiv \int d^2\hat{R}\ \Phi^B(\vec{R})$$

$$\left( \frac{\langle \Phi^{BO^+}(R) | H | \Phi^{BO^+}(R) \rangle}{\langle \Phi^{BO^+}(R) | \Phi^{BO^+}(R) \rangle} \right)_{最小値} = -52.069 \ \mathrm{MeV}$$

差 2.379 MeV

変形凝縮状態 $\Phi^{0^+}_{I}$ $-54.448$ MeV

◎ $R_j = 0.5 \times j$ fm $j = 1 \sim 23$

最小エネルギー $-54.444$ MeV

$$|\langle \Psi^{0^+}_{最小} | \Phi^{0^+}_{I} \rangle|^2 = 0.9973$$

◎ $R_j = 0.5 \times j$ fm $j = 1 \sim 24$

最小エネルギー $-54.446$ MeV

$$|\langle \Psi^{0^+}_{最小} | \Phi^{0^+}_{I} \rangle|^2 = 0.9980$$

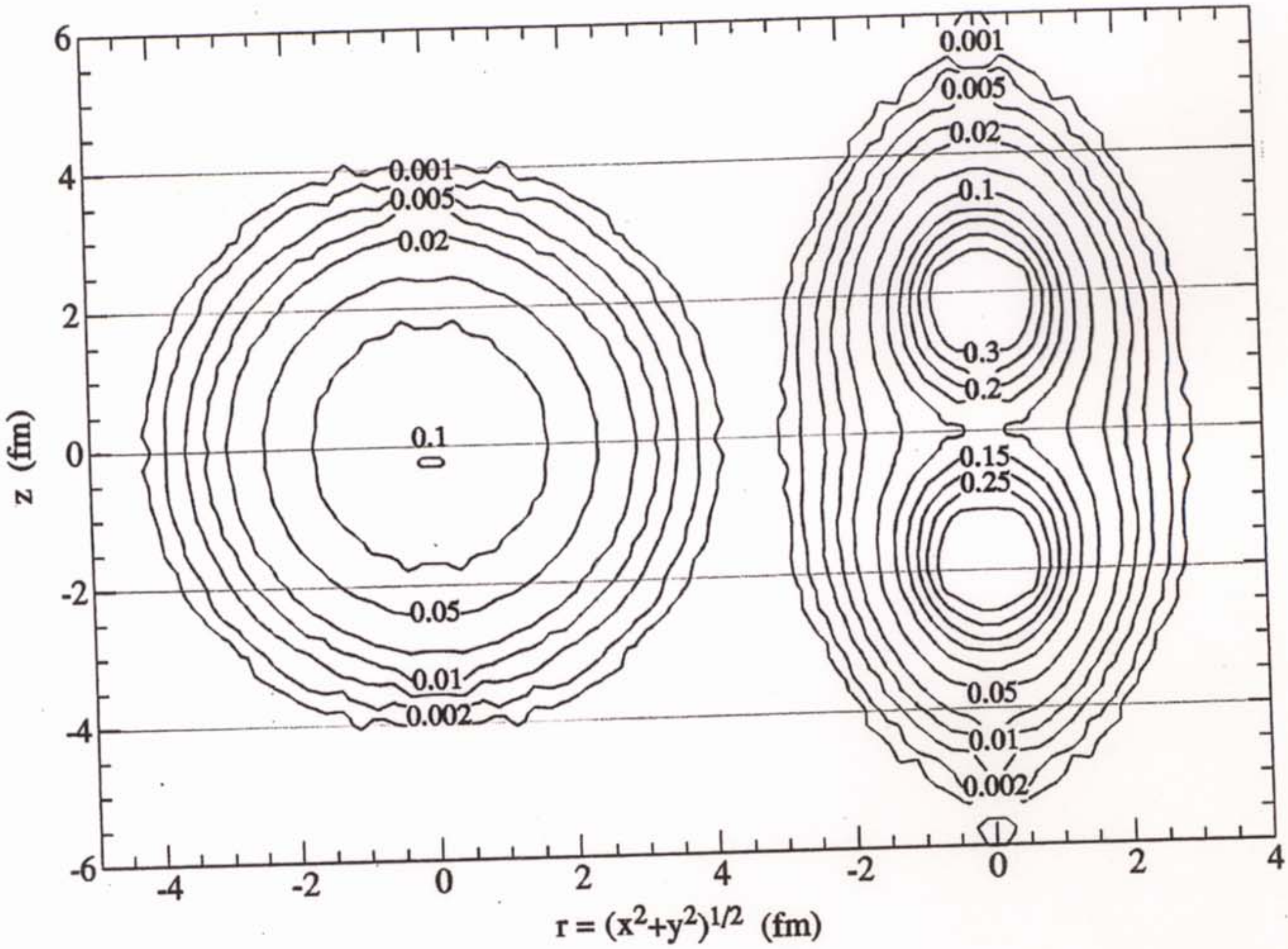


FIG. 15. Contours of constant density, plotted in cylindrical coordinates, for $^8$Be($0^+$). The left side is in the ‘‘laboratory’’ frame while the right side is in the intrinsic frame.

Phys. Rev. C 62, 014001 (2000)

# Threshold states

weak binding　　希薄密度
(gas-like)

◎ クラスター状態

* $n\alpha$ threshold

$\alpha$ = Bose 粒子　　Bose 凝縮

* その他の cluster threshold
( Ikeda diagram)

◎ 中性子過剰核

* weak binding neutrons

* di-neutron = Bose 粒子

di-neutron 自体が
ゼロエネルギー結合で大きく広がっている
( $\alpha$ とは異る)

# E0 strength in $^{12}C$ measured in the (p,p¢) reaction

*M.A. de Huu, C. Bäumer [a)], A.M. van den Berg, D. Frekers [a)], M. Hagemann [b)], M.N. Harakeh, V.M. Hannen, J. Heyse [b)], E. Jacobs [b)], M. Mielke [a)], S. Rakers [a)], R. Schmidt [a)], H.J. Wörtche, for the EuroSuperNova collaboration*

Although $^{12}C$ is a well studied nucleus, there are still many open questions about its structure. Especially the situation with regard to the E0 strength distribution below 15 MeV excitation energy is not yet clear. In nuclear data compilations [1], a strength concentration around $E_x$ = 10.3 MeV has been tentatively assigned to be $0^+$. During the data taking period of March 2000 and June 1999, the $^{12}C$(p,p¢) reaction has been studied at beam energies of 150 and 172 MeV, at angular settings of the Big-Bite Spectrometer (BBS) between 4° and 18° and between 5° and 25°, respectively on a 9.1 mg/cm$^2$ $^{12}C$ target. The scattered protons were momentum analyzed with the BBS using the EuroSuperNova focal-plane detection system.

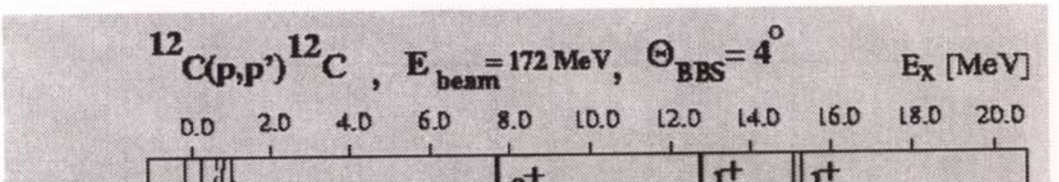


**Figure 1:** ***Energy spectrum of $^{12}C$ measured at a beam energy of 172 MeV.***

The energy spectrum at a BBS setting of 4° is shown in figure 1. The cross sections for the elastic channel and the first-excited state ($E_x$ = 4.439 MeV) at a bombarding energy of 150 MeV are consistent with earlier measurements performed at IUCF and Orsay (see figure 2). The cross sections for the first excited $0^+$ at $E_x$ = 7.654 MeV and the bump at $E_x$ = 10.3 MeV at a beam energy of 172 MeV are plotted in figure 2. The similarity of the angular distributions points to a monopole assignment of the 10.3 MeV bump, in good agreement with Ref. [2].

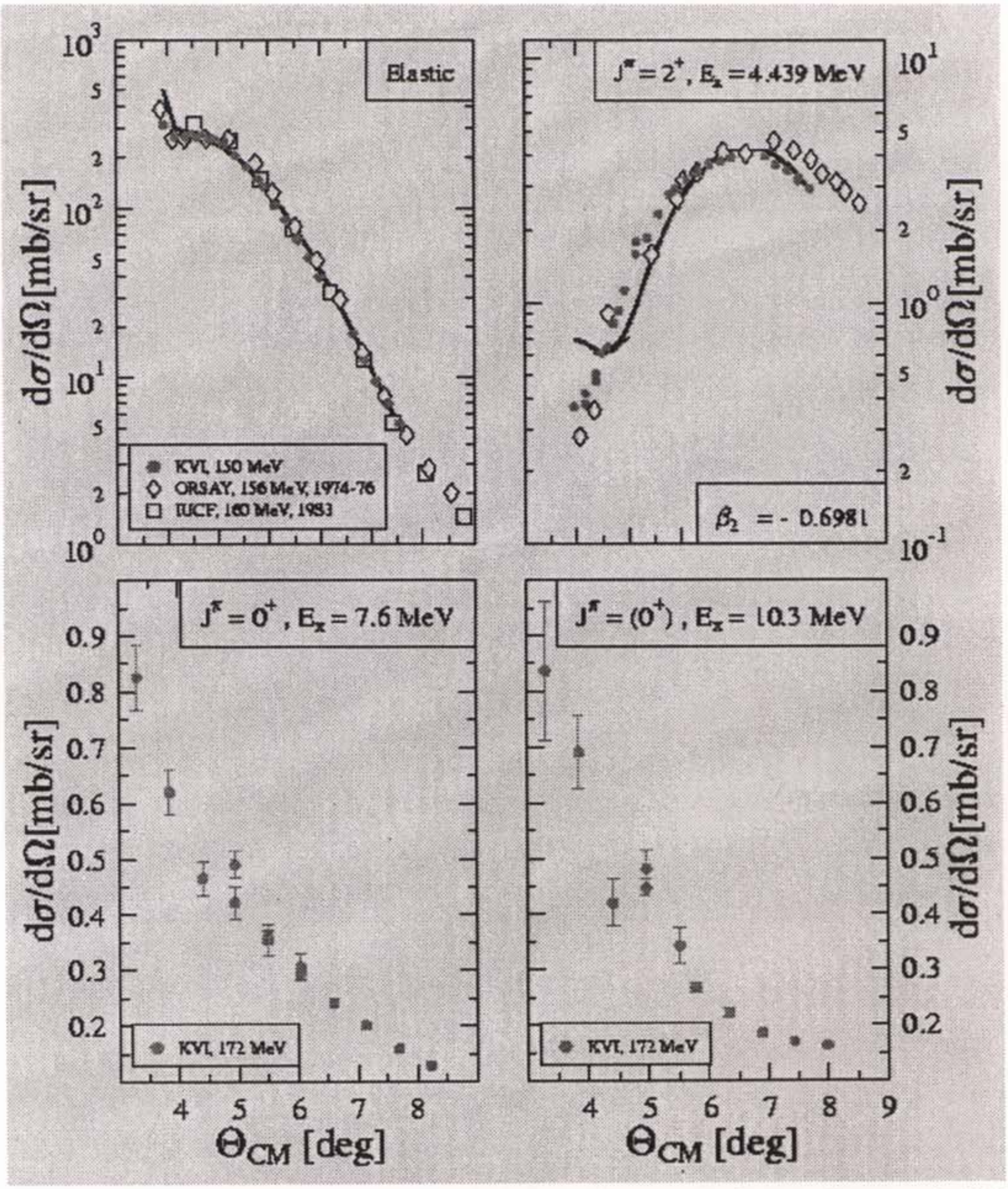


**Figure 2:** ***Cross sections for the ground state, first-excited state, first-excited $0^+$ and the 10.3 MeV bump in $^{12}C$; data (dots, triangles and diamonds) are compared with CCBA calculations (solid lines).***

Coupled-channels calculations using the computer code chuck are being performed to extract the strength of these $0^+$ states. Preliminary results from the calculations are shown in figure 2 for the elastic channel and the first-excited $2^+$ state.


a) Institut für Kernphysik, Universität Münster, Germany.
b) Vakgroep Subatomaire en Stralingsfysica, Universiteit Gent, Belgium.



[1] F. Ajzenberg-Selove and C.L. Busch, Nucl. Phys. **A336**, 1 (1980).
[2] W. Eyrich *et al.*, Phys. Rev. C **36**, 416 (1987).